

# On the Development of a Full-Scale Numerical Towing Tank *Reynolds Scaling Effects on Ducted Propellers and Wakefields*

Norbert Bulten<sup>1</sup>, Maarten Nijland<sup>2</sup>

<sup>1</sup>Wärtsilä Industrial Operations, Global R&D, Drunen, The Netherlands

<sup>2</sup>Wärtsilä Ship Power, Application Technology, Drunen, The Netherlands

## ABSTRACT

Continuously increasing computer power has made it nowadays possible to make performance calculations based on RANS CFD method for propellers within commercial acceptable lead times. Wärtsilä has decided to extend the scope of the numerical analyses to also include the ship hull geometry. The final goal is to have a full scale numerical towing tank in operation within the next few years. This ambitious plan can be divided into several building blocks; like developing a method to calculate open water performance and the implementation of the cavitation model.

In this paper, two building blocks will be discussed in more detail. The first topic is about the Reynolds scaling effects on ducted propellers, like the well-known 19A-nozzle. The performance of the propeller and nozzle are split into pumping efficiency and loss-coefficients. Comparison of model scale and full scale calculations give a clear explanation of the scaling effects observed. The second topic is the method to calculate wakefields. It is confirmed once more that there are clear scaling effects on the wakefields as well.

## Keywords

CFD, propulsion, propeller, nozzle, wakefield

## 1 INTRODUCTION

A towing tank has been a well-known testing environment in marine industry since the end of the 19<sup>th</sup> century. Developments in computational fluid dynamics (CFD) in the last decade have opened up a completely new approach in the marine research world. Based on the ongoing developments, both on computing power and improved numerical models, Wärtsilä decided some years ago to start a program to develop a full-scale numerical towing tank based on the available commercial CFD software from CD-adapco (Star-CD and Star-CCM+).

Three different challenges can be recognized in this ambitious project: first of all, a good accuracy of the numerical method on model scale has to be obtained. This means getting good agreement between CFD calculations

and the available experimental model scale data. The second challenge is the determination of the validity of the full-scale CFD results. This means in general that the Reynolds scaling effects as found in the calculations have to be explained by logic reasoning, due to a lack of proper full-scale measurement data. Detailed analysis of the CFD results both on model scale and full scale in combination with basic fluid dynamics and physics should give indications about the actual occurring flow phenomena. Once these are understood, confidence in the full-scale results can grow. The third challenge will be the possibility to develop completely new ways of describing the interaction effects between ship hulls and propellers. The standard methodology of combining hull resistance, propeller open water and a self-propulsion test, which gives interaction factors like wake fraction, thrust deduction and relative rotative efficiency might not be suitable for all hull forms and propulsion types. Based on quantifiable flow field parameters, like flow through a ducted propeller, other ways of so-called "hydrodynamic book-keeping" might evolve.

Since the process of detailed analysis of the flow is much more time consuming than the actual calculation, the complete implementation of all the building blocks of the full-scale numerical towing tank has not yet been finished. Nevertheless, several interesting intermediate results can be presented.

Figure 1 shows the various building blocks of the numerical self-propulsion test. As can be seen in Figure 1, the open water performance calculations of all types of propulsion units, e.g. open and ducted propellers, azimuthing thrusters and propellers with integrated rudders are in place and their results can be exploited. The methodology to calculate wakefields has also been developed. Work on the implementation of the cavitation model is still in progress, though results of the validation work and results of some initial calculations on propellers are available (Oprea 2011). In the following sections these three topics will be discussed in more detail.



**Figure 1: Building blocks of a full-scale numerical towing tank**

## 2 OPEN WATER PERFORMANCE

Calculations of the open water performance can be split into various propulsor types. In this paper, the focus will be mainly on the open water calculations of ducted propellers. In the following section, a comparison will be presented between the CFD results of model scale calculations and the well-known published experimental data from Marin (Kuiper 1992). As will be shown in Section 2.2, clear differences are found in the CFD results for model scale and full scale. This seems to be a contradiction to the commonly accepted practice that no Reynolds scaling effect is applied when extrapolating model tests with ducted propellers. In order to get a better understanding of the physical phenomena, a method is introduced that splits the performance of the ducted propeller in some loss-coefficients and a pump-efficiency, as used in common pumping theory. Based on this analysis, a clear scale effect of the pump efficiency is found, which is in line with available literature.

### 2.1 Validation of Kaplan propeller in 19A

For the validation of the RANS-CFD method for ducted propellers the performance of various propellers in

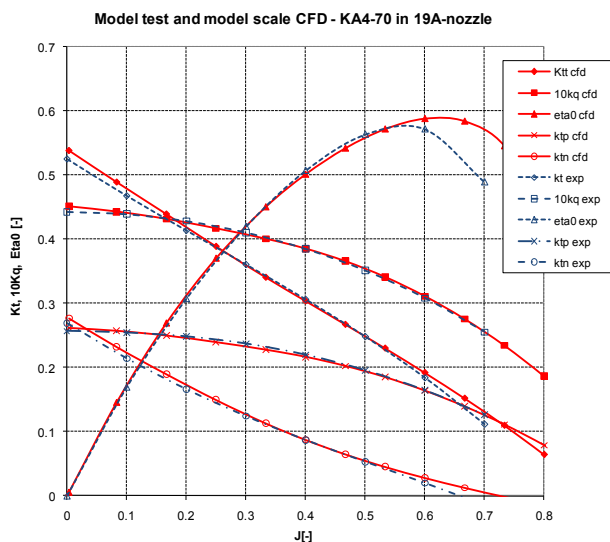


**Figure 2: Comparison of measured and calculated open water performance of Kaplan 4-70 propeller in 19A nozzle**

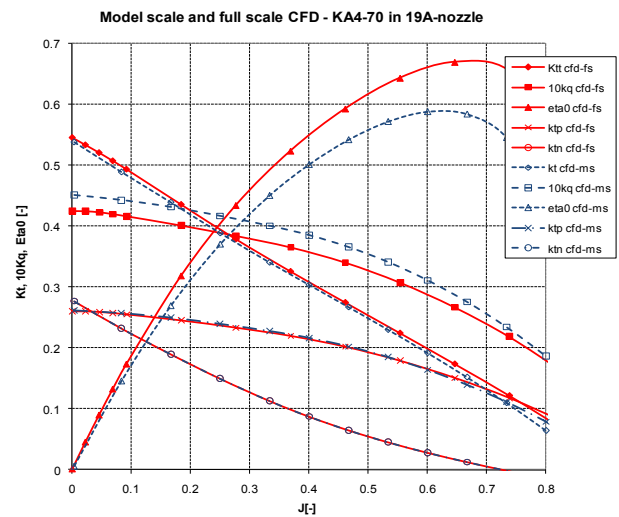


**Figure 3: Comparison of calculated open water performance of Kaplan 4-70 propeller in 19A nozzle on model scale and full scale**

different nozzles has been calculated. In this section, the CFD results of a Kaplan 4-70 propeller in 19A nozzle are compared with the available experimental data (Oosterveld 1973).

Figure 2 shows the comparison for the propeller thrust and torque as well as the nozzle thrust and the overall efficiency. A very good agreement is found from bollard-pull condition up to the maximum efficiency. At extreme high  $J$ -values a deviation is seen, but this is to be neglected since the measured points are subjected to inaccuracies due to the low nozzle thrust, and above all, these operating points are not of interest.

### 2.2 Reynolds scaling effect on 19A-nozzle

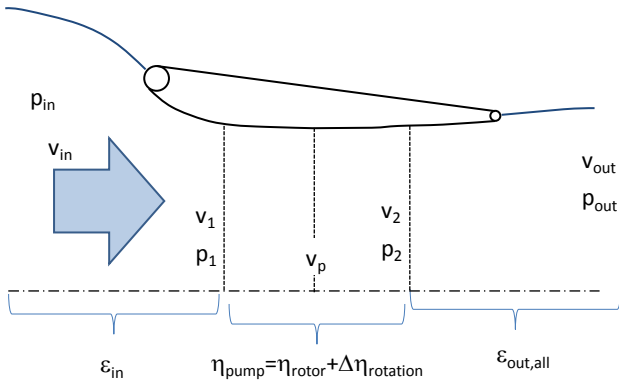
Given the fact that the viscous effects are taken into account in the RANS-CFD calculations, it is expected that the results for model scale and full scale will give differences, as observed before by others (Abdel-Maksoud & Heinke 2002, Mertes & Heinke 2008).

Figure 3 shows the comparison of model scale and full scale CFD results for the Kaplan 4-70 propeller. The differences in open water efficiency and torque can be clearly seen. On the other hand, the propeller and nozzle thrust are almost identical for model scale and full scale.

Explanation for the behavior of thrust and torque might be due to the presence of two different phenomena: (1) due to the Reynolds scaling, the propeller performance will change in line with the behavior as observed for open propellers. This means small reduction of torque and small increase of thrust. For a ducted propeller there is a second effect however: (2) due to the lower viscous losses on full scale, the flow rate through the nozzle will increase which results in a reduced loading on the propeller. So, both torque and thrust will reduce slightly.

### 2.3 Method to determine pump-efficiency and loss coefficients

The theoretical idea as presented in the previous section can be analyzed in more detail within the CFD program.



**Figure 4: Sketch of parameters used in ducted-propeller post-processing**

Therefore, not the standard open propeller theory is used, but instead, the ducted propeller is treated as an axial pump. For the inflow to the propeller, a certain loss-coefficient can be defined. For the exit loss, two coefficients are defined to account for the axial losses and the tangential losses separately. The performance of the propeller is based on the total pressure rise, often denoted as pump head.

Figure 4 shows a sketch of the system as used for the post-processing of the CFD results. The dividing streamline is sketched for indication. It should be noted that the dividing streamline at the inlet side is strongly related to the loading condition.

The viscous loss-coefficient at the inlet side is defined as:

$$\varepsilon_{in} = \frac{P_{in} + \frac{1}{2} \rho v_{in}^2 - p_1 - \frac{1}{2} \rho v_1^2}{\frac{1}{2} \rho v_p^2} \quad (1)$$

where  $p$  is the static pressure,  $\rho$  the density and  $v$  the velocity. The subscripts denote the various locations, *in* is far upstream or downstream, 1 is inside the nozzle upstream of the propeller and *p* is at the propeller definition plane.

For the exit loss, the equations are slightly more complex since the effects of rotational losses and axial losses have to be decoupled. The method to achieve this is to calculate the total pressure with and without the effects of the tangential velocity:

$$\begin{aligned} p_{T-all} &= p_{stat} + \frac{1}{2} \rho (v_{ax}^2 + v_{tg}^2 + v_{rad}^2) \\ p_{T-ax} &= p_{stat} + \frac{1}{2} \rho v_{ax}^2 \end{aligned} \quad (2)$$

where  $p_T$  is the total pressure,  $v_{ax}$  the axial velocity,  $v_{tg}$  the tangential velocity and  $v_{rad}$  the radial velocity.

It should also be noted that the radial velocities are neglected inside the nozzle. The two types of total pressure integrals just aft of the propeller can be used both in the calculation of the pump efficiency:

$$\eta_{pump} = \frac{\rho g H Q}{P} = \frac{(p_{T2} - p_{T1}) \cdot Q}{P} \quad (3)$$

where  $\eta_{pump}$  is the pump efficiency,  $H$  is the pump head,  $Q$  the flowrate and  $P$  the shaft power.

The difference in pump efficiency based on the two methods to determine the total pressure  $p_T$  is denoted as the efficiency loss due to rotation.

In order to be able to compare the results of propellers with different P/D-ratios, all graphs in the following section are based on the so-called jet-velocity ratio  $\mu$ .

$$\mu = \frac{v_{in}}{v_{out}} \quad (4)$$

Usage of the jet-velocity ratio has some advantages: by definition, the bollard pull condition is at  $\mu=0$  and the condition where the total thrust, and therefore the efficiency is zero, is at  $\mu=1$ . Besides the variation of propeller pitch, various nozzles have also been studied to check the sensitivity on duct geometry in this research project. In order to quantify some effects related to the nozzle exit geometry, a second velocity ratio is introduced: the outlet velocity ratio  $\lambda$ . In case of a cylindrical aft section of the nozzle, this ratio is close to 1.0; in case of a diffuser exit type, the ratio can increase to typically 1.1 – 1.2.

$$\lambda = \frac{v_p}{v_{out}} \quad (5)$$

The two velocity ratios  $\mu$  and  $\lambda$  can be used to rewrite the standard momentum theory thrust equation:

$$T = \rho Q (v_{out} - v_{in}) = \rho Q v_p \left( \frac{1 - \mu}{\lambda} \right) \quad (6)$$

At first glance it may seem that  $\lambda$  larger than 1.0 would have negative effect on the thrust. This is not the case for many interesting conditions, like bollard pull situation. In such condition, it can be proven that the flow rate  $Q$  through the nozzle will increase sufficiently to eventually lift up the bollard pull thrust.

## 2.4 Analysis of pump-efficiency and loss coefficients

In this section, the results of some typical coefficients and efficiencies will be shown.

Figure 5 shows the inlet loss coefficient for propellers with different P/D-ratios in a 19A nozzle. For the various propellers, the same trend is found for the inlet loss-coefficient. This is in line with the expectations, since the flow at the inlet and upstream of the nozzle is more or less similar for propellers at given jet velocity ratio  $\mu$ .

The trends for other nozzles, like 37 and HR are comparable, though subtle differences have been found. Comparison of the loss-coefficients for model scale and full scale learns that the losses on model scale are in general a bit larger. This can be attributed to the lower Reynolds number on model scale.

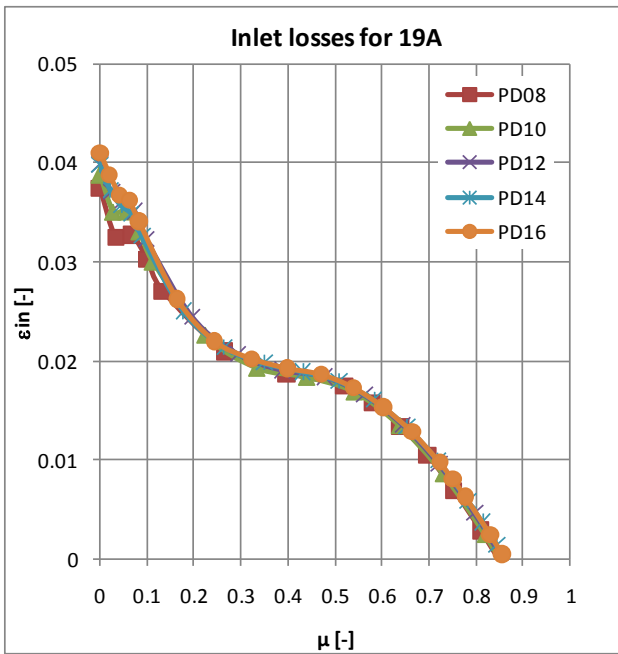


**Figure 5: Inlet loss-coefficient  $\epsilon_{in}$  for different propellers in 19A nozzle**

The insensitivity to nozzle shape and propeller pitch, as found for the inlet loss-coefficient, will most probably not be found for the rotational and exit-losses.

Figure 6 shows the rotational loss, based on the difference in pump efficiency with and without the tangential velocity component as discussed in the previous subsection. A clear relation to the propeller pitch can be recognized. This trend is not seen in Figure 7, where the pump efficiency for various propellers is shown. Above a P/D ratio of about 1.0, the pump efficiency is more or less constant over the important range of jet-velocity ratios, as well as P/D-ratios. In order to get good system efficiency, the pump efficiency should be optimized, whilst keeping

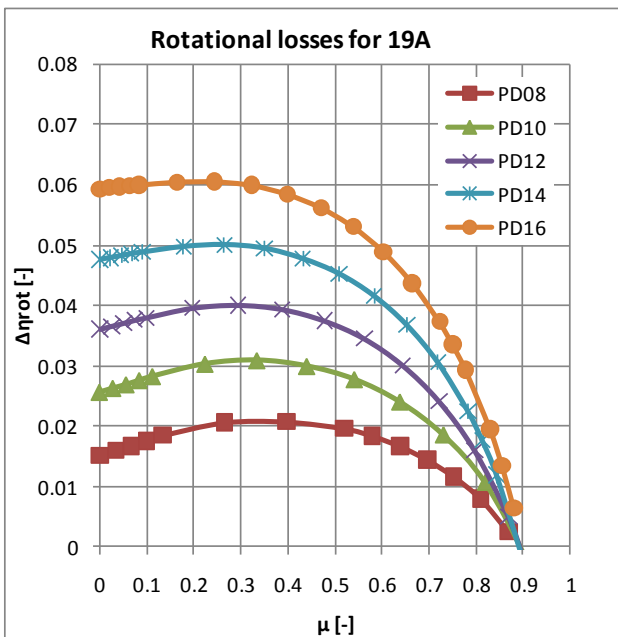


**Figure 6: Rotational loss for different propellers in 19A nozzle**

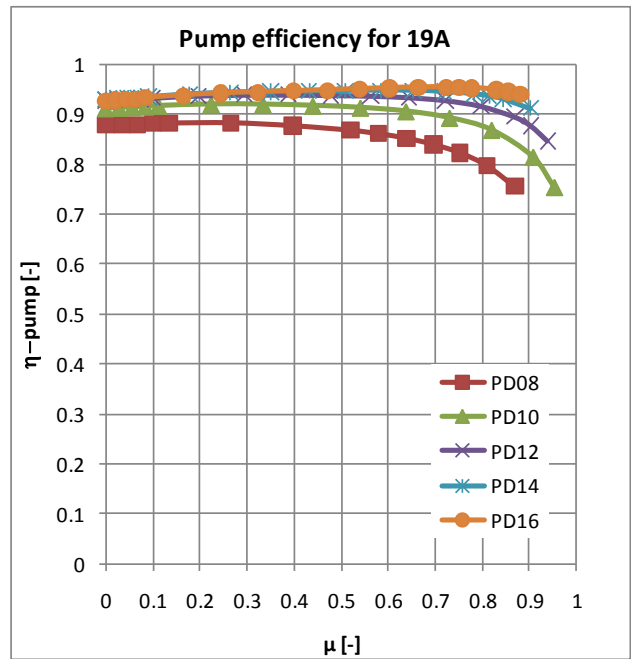


**Figure 7: Pump efficiency for propellers with different P/D-ratios in 19A-nozzle**

the losses to an acceptable level.

A complete overview of the various loss coefficients is shown in Figure 8 for the complete operating range. The net open water efficiency of the system is shown as well. A detailed review of this chart shows that for some regions there are no inlet losses shown. This is supposed to be related to the way the various loss-coefficients have been defined. This way of representation clearly shows which of the various loss coefficients are responsible for the obtained open water efficiency.

### Loss coefficient overview

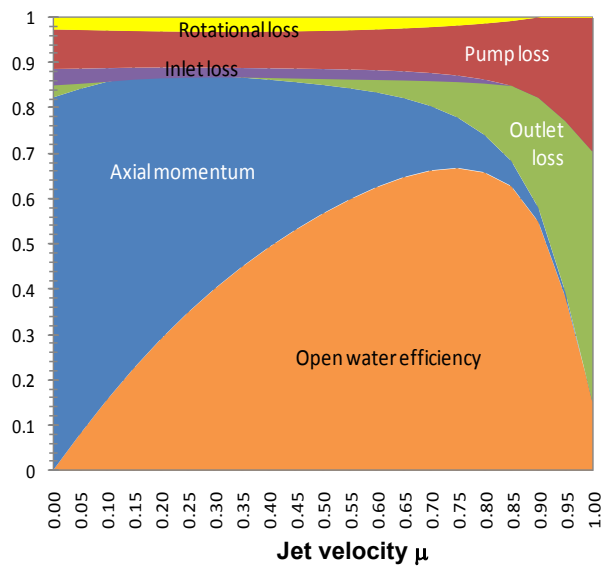


**Figure 8: Overview of all loss coefficients over jet velocity range  $\mu$**

In addition to this there has been derived a relation between the propeller open water efficiency and the various loss coefficients:

$$\eta_0 = \frac{2\mu(1-\mu)}{1-\mu^2 + \lambda^2(\varepsilon_{in} + \varepsilon_{out,all})} \cdot \eta_p \quad (7)$$

In case it would be possible to design a propulsion system for given jet velocity ratio  $\mu$  by playing with the designs parameters, the open water efficiency can be tuned. In waterjet propulsion systems this is already achieved by selecting the proper nozzle exit diameter (Bulten, 2006).

For the prediction of the bollard pull a similar type of equation can be derived, based on the Merit coefficient definition:

$$MC = \frac{(K_t/\pi)\lambda^{3/2}}{Kq} = \frac{2(1-\mu)^{3/2} \cdot \lambda^{1/2} \cdot \eta_p}{1-\mu^2 + \lambda^2(\varepsilon_{in} + \varepsilon_{out,all})} \quad (8)$$

At bollard pull, where  $\mu=0$ , equation 8 reduces to:

$$MC|_{j=0} = \frac{2 \cdot \lambda^{1/2} \cdot \eta_p}{1 + \lambda^2(\varepsilon_{in} + \varepsilon_{out,all})} \quad (9)$$

Equation 9 shows that  $\lambda$  larger than 1.0 can be beneficial for the bollard pull, as long as the loss-coefficients remain small.

### 2.5 Nozzle scaling effects

The method to split the available power in net power and various loss coefficients has been applied to the full scale CFD results as well. In Figure 9, the comparison of pump efficiency on model scale and full scale is shown. This diagram shows the difference in pump efficiency, which is in line with existing textbooks on axial-pump theory

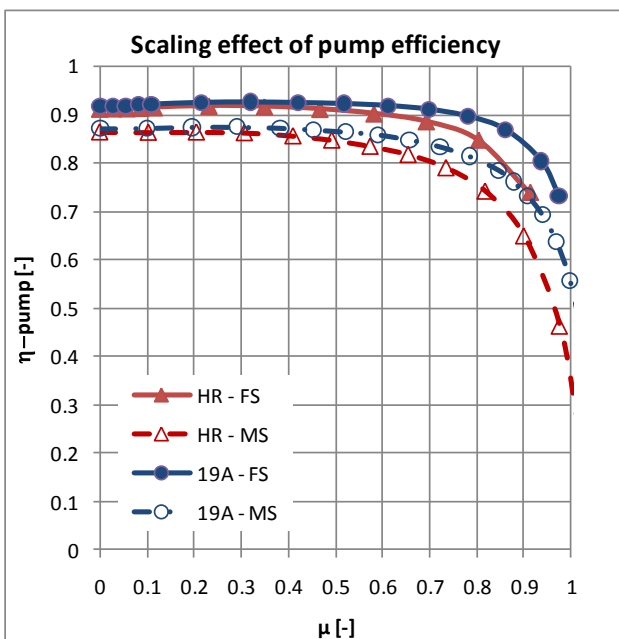


Figure 9: Comparison of pump efficiency for model scale and full scale for 19A and HR nozzle

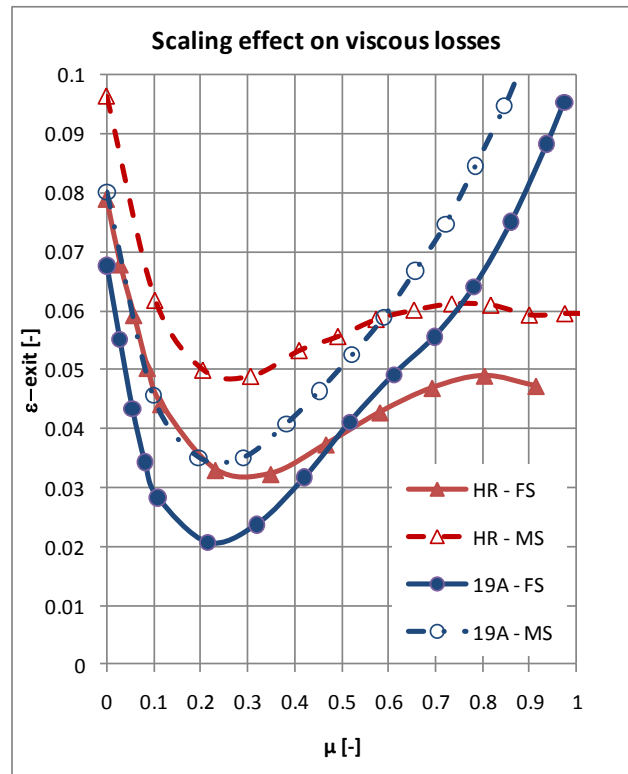


Figure 10: Comparison of loss coefficients for model scale and full scale for 19A and HR nozzle

(Pfleiderer 1961).

The viscous losses as shown in Figure 10 clearly confirm the expectations of larger losses at model scale compared to full scale.

Based on the analysis presented in this section it can be concluded that the pump efficiency on model scale will be lower than the full scale efficiency. In addition to this, the viscous losses will be slightly larger at model scale. Consequently, the dimensionless flow rate through the nozzle will be larger on full scale compared to model scale. The increase in flow rate will lead to a lighter running propeller, and thus to a lower propeller torque and thrust. Combined with the conventional Reynolds scaling methods for propeller blades, which gives an increase of thrust and a decrease of torque, the result as shown in Figure 3 is explained. The fact that the two phenomena cancel each other on the propeller thrust should be regarded as coincidence, rather than as an indication of the lack of Reynolds scaling in ducted propellers.

### 3 WAKEFIELD CALCULATIONS

Another building stone in the development of the full-scale numerical towing tank is the methodology to calculate wakefields. With this term, the velocity distribution at the propeller location for a bare hull configuration is meant. This inflow velocity is important input data for the propeller design process, mainly because of the non-uniform character of the velocity distribution.

Before numerical methods were available, wakefields were measured in model scale tests. Since this process is rather time consuming and costly, often no wakefield measurements are carried out, which leaves the propeller designer no other option than to make an educated guess of the wakefield based on other, though similar shaped vessels. The numerical method has been developed to provide a method which can be used to calculate a wakefield for any given vessel within commercial reasonable time and cost. The time saved with the method, compared to the conventional model scale measurements, can be used in the propeller design process to further optimize the design, for example.

A second important topic which can be addressed with the numerical method is the analysis of the differences in wakefield between model scale and full scale. Based on full scale observations of the cavity pattern on various propellers, it has been concluded that the use of a so-called full scale wakefield in the propeller design software gives much better agreement (Ligtelijn et al 2004).

### 3.1 Implementation of the method

The hull geometry is provided as 3D-CAD data. The meshing is based on the methodology with a thin extrusion layer near the hull surface and a structured trimmed mesh in the remainder of the domain. In order to control the boundary layer development, the thickness of the first cell is prescribed to be a fixed value. In line with the propeller performance calculations within Wärtsilä, the boundary layer development is captured with aid of wall functions. The  $y^+$  values are in general within the range of 100 to 300. In the development phase of the project, the effects of several turbulence models have been verified, and it could be confirmed that the use of the standard  $k-\epsilon$  turbulence model gives reliable answers. Since this turbulence model is used for the propeller performance and propeller-hull interaction research, there is a preference to keep as much as possible numerical consistency.

In order to reduce the calculation time it, has been decided to apply a symmetry plane boundary condition at the free-surface plane within this version of the wakefield calculation method. In future versions however, it is planned to take the wave making effects into account as well, though they are expected to have a small effect on the actual wakefield. Based on the current settings, the calculations are performed with a steady solution method. This results in overall calculation times which are very acceptable for commercial use.

### 3.2 Validation of the method

The validation of the wakefield calculations can be done on various levels. Obviously, one can make a detailed comparison of the measured and calculated velocity components. In such a comparison the accuracy of the measurements will also play a role. Figure 11 shows the comparison of a measured and calculated wakefield on model scale. The main trends of the velocity distribution are captured quite well within the calculations.

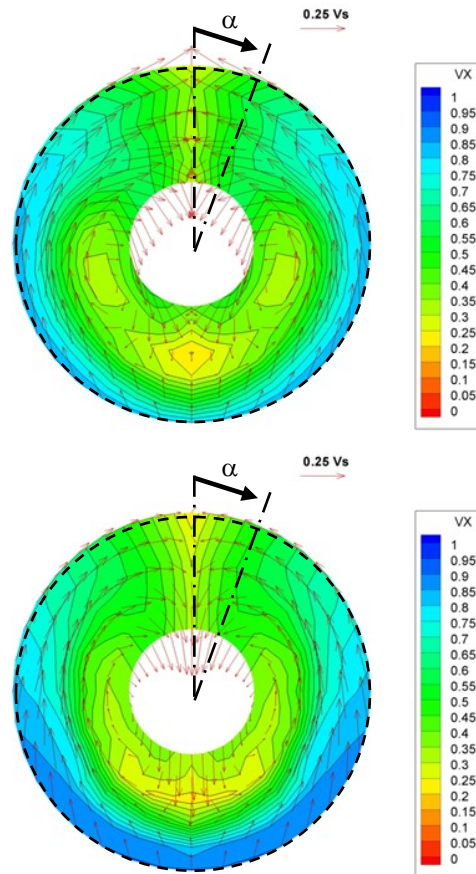


Figure 11: Comparison of measured (top) and calculated wakefield on model scale

The largest differences are found at the outer radii in the lower part (section from 135 to 225 degrees). In this section, the hydrostatic pressure is largest, which reduces the risk for cavitation.

Table 1: Wake fraction comparison

	Measured	CFD Model scale	CFD Full scale
Wake fraction	0.5132	0.5041	0.3477

Evaluation of the wake fraction, as presented in Table 1, shows that the agreement between measurements and model scale CFD calculations is excellent, certainly when it is related to the difference between model scale and full scale calculations. The results of the full scale calculation will be discussed in more detail in the next subsection. To avoid the discussion about the significance of the deviations in the velocity field, it has been decided to use the measured and calculated wakefields in the propeller design process. The typical design criteria, i.e. power absorption, cavity extent and pressure pulses have been determined for both wakefields. The calculated cavity extend in the top section is shown in Figure 12, where the measured and calculated wakefields are used in the propeller design process. Agreement between the two sets is good, which gives another, implicit validation of the wakefield calculation applicability.

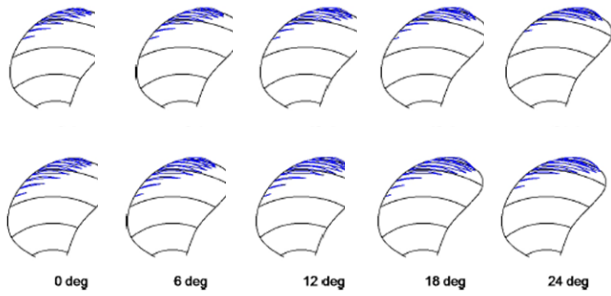


**Figure 12: Comparison of calculated cavity extent based on measured (top) and calculated wakefield on model scale**

### 3.3 Reynolds scaling effects

As shown in Table 1, a significant difference between the model scale and full scale wake fraction is found. This is a result of the difference in the boundary layer development along the hull. At model scale, the relative thickness of the boundary layer is larger compared to the full scale boundary layer. This phenomenon is responsible for the lower viscous friction at full scale. A thinner boundary layer at full scale also gives a lower velocity deficit in the propeller plane, which results in a lower nominal wake fraction.

The significant difference in nominal wake fraction is a potential point of discussion, since it will have an effect of the effective wake fraction, as determined in a self-propulsion test. Consequently, there will be an effect on the prediction of the hull efficiency, defined as:

$$\eta_{hull} = \frac{(1-t)}{(1-w)} \quad (10)$$

where  $\eta_{hull}$  is the hull efficiency,  $t$  the thrust deduction and  $w$  the effective wake fraction. This hull efficiency is an important factor in the overall propulsive efficiency  $\eta_D$ :

$$\eta_D = \eta_{hull} \cdot \eta_r \cdot \eta_0 \quad (11)$$

where  $\eta_r$  is the so-called relative rotative efficiency, which is in general very close to 1. If the full scale wake fraction is lower than the model scale value, this will result in lower hull efficiency, based on Equation 10. The present method opens possibilities to quantify the wake scale effect more precisely, as an alternative for the usually statistics-based corrections in extrapolation methods.

## 4 CONCLUSIONS AND OUTLOOK

The use of CFD in marine industry has resulted in a clear increase of understanding of all kinds of phenomena. It is acknowledged that many empirical values which have been based on model scale testing need to be discussed and disputed based on this full scale CFD data.

Given the good correlations with model scale measurements, the results are suitable for further detailed analysis. This possibility to perform detailed analyses is one of the key features of the added value of CFD methods.

In this paper, the Reynolds scaling effect, which is present on ducted propellers, has been identified and explained based on the theory of loss coefficients and pump efficiency. The findings regarding scaling of axial pump efficiency are in agreement with literature.

The new method to analyze ducted propellers can also be used to identify the sensitivity of the various loss coefficients occurring in the propulsion system on the design operating condition. Propulsion designs for free-sailing conditions will have a different optimum design than bollard pull units.

The presented method will be applied to numerical self-propulsion calculations as well in the near future to determine propeller-hull interaction in a different way. The conventional method, based on wake fraction, thrust deduction and relative rotative efficiency, does not always give clear trends for ducted propellers.

The wakefield calculation method has been implemented successfully. Use of this method will give the propeller designer improved input data, especially if there have not been performed any wakefield measurements. In addition, it provides the possibility to design directly in a full scale wakefield. Given the significant scaling effects, the conventional wake fractions will be subjected to discussions in the future. The wakefield calculation method will be used in the propeller design process within Wärtsilä from now on.

The next step in the CFD program to develop the full scale numerical towing tank will be the implementation of the free surface effect, as shown in Figure 1.

## ACKNOWLEDGEMENTS

The contributions to this work of the CFD-Propulsion team of Wärtsilä Global R&D are highly appreciated.

## REFERENCES

- Abdel-Maksoud, M. & Heinke, H.-J. (2002). 'Scale effects on ducted propellers'. 24th Symposium on Naval Hydrodynamics, Fukuoka, Japan
- Bulten, N.W.H. (2006). Numerical analysis of waterjet propulsion system. PhD Thesis, Technical University of Eindhoven.
- Kuiper, G. (1992). 'The Wageningen Propeller Series'. Marin Publication, pp. 92-001.

- Ligtelijn, J. T., Wijngaarden, H. C. J. van, Moulijn, J. C. & Verkuyl, J. B. (2004) 'Correlation of Cavitation: Comparison of Full-Scale Data with Results of Model Tests and Computations'. Transactions of the Society of Naval Architects and Marine Engineers **112**, pp. 80-110.
- Mertes, P. & Heinke, H-J. (2008). 'Aspects of the Design Procedure for Propellers Providing Maximum Bollard Pull'. Proceedings ITS-2008, Singapore.
- Oosterveld, M.W.C. (1973). 'Ducted propeller characteristics'. RINA Symposium on Ducted Propellers, London.
- Oprea, I. (2011). 'Analysis of cavitating flow in tunnel thruster'. RINA Conference: Developments in Marine CFD, pp. 143-152.
- Pfleiderer, C. (1961) Kreiselpumpen. 5<sup>th</sup> ed. Springer Verlag.